

INTERFEROMETRIC MEASUREMENT OF ACCELERATION AT RELATIVISTIC SPEEDS

PIERRE CHRISTIAN AND ABRAHAM LOEB
ASTRONOMY DEPARTMENT, HARVARD UNIVERSITY, 60 GARDEN ST., CAMBRIDGE, MA 02138

Draft version October 8, 2018

ABSTRACT

We show that an interferometer moving at a relativistic speed relative to a point source of light offers a sensitive probe of acceleration. Such an accelerometer contains no moving parts, and is thus more robust than conventional "mass-on-a-spring" accelerometers. In an interstellar mission to Alpha-Centauri, such an accelerometer could be used to measure the masses of exoplanets and their host stars as well as test theories of modified gravity.

1. INTRODUCTION

The Terrell effect (Terrell, J. 1959; Penrose, R. 1959) implies that a spherical source will always appear circular to a moving camera, in seeming contradiction to the naive expectation from Lorentz contraction in special relativity. In addition, for the simplest case of a sphere that extends across a small solid angle, the sphere will appear rotated.

Following this realization, much work has been done in generalizing the Terrell effect to cases where the solid angle is not necessarily small. It was found that while the spherical source is still viewed as a circle, more complex transformations than rotations are required to map the surface of the sphere to the one in the photographic plane (Hollenbach, D. 1976; Suffern, K. 1988; Scott, G. D. and van Driel, H. J. 1970). Here we will restrict our attention to the simple case of a small solid angle, and focus on the temporal aspect of the Terrell effect. Even if the sphere is not featureless, one cannot infer whether the sphere is moving and Lorentz contracted or stationary but merely rotated just by taking a snapshot of it using a conventional camera. However, each point in the photographic plane can be traced back to the source through null geodesics. Due to the finite speed of light, geodesics corresponding to different points in the circular photograph travel for differing amounts of time. The timing information encoded by each light ray conveys the true nature of the sphere's motion.

Whereas previous considerations of the temporal Terrell effect were based on an abstract construction involving a lattice of clocks (Sheldon, E. 1989), we propose a more natural way to detect the temporal Terrell effect based on interferometry, where the temporal information is encoded in phase measurements of light. In addition, we show that the temporal Terrell effect allows a measurement of acceleration with high precision due to a relative motion between the source and the camera.

Recently, an interstellar travel mission, *Breakthrough Starshot* (Breakthrough Starshot 2016), was initiated. The project aims to send a large number of gram mass microchips equipped with cameras to the nearest star system, Alpha-Centauri (4.2 light years away from Earth), at 20% the speed of light. These microchips will aim to take close-up images of the planets in the star system. Furthermore, if during the travel these chips

emit light pulses at known intervals, they can be used as standard-clock beacons much like pulsars. A passing gravitational wave will modulate the time between pulses, allowing the detection of long wavelength gravitational radiation.

One other science benefit of such a mission could be to measure the masses of both exoplanets and their host stars as well as to test theories of modified gravity. Launching a spacecraft to a relativistic speed, however, requires a high acceleration that could potentially damage conventional mechanical accelerometers. A feasible alternative is to use the Doppler shift of the signal between the spacecraft and Earth to measure the accelerations. However, the total shift in speed for a spacecraft passing at 0.2c at a distance of 1 AU from an Earth mass planet is $\sim 4 \times 10^{-3} \text{ cm s}^{-1}$. The best Doppler sensitivity for bright stars is 4 orders of magnitude weaker (Schneider et al. 2011) and it is difficult to imagine performance that is much better for a source that is much fainter than a star.

In particular, an Earth-mass planet was recently discovered in the habitable zone (11.2 days orbit) around Proxima Centauri, a $0.12M_{\odot}$ star in the three-star system of Alpha Centauri (Anglada-Escude, G. et al 2016). The radial velocity technique by which the planet was detected allows to set only a minimum value on its mass, 1.3 Earth masses. Using a fleet of spacecrafts equipped with cameras and laser communication devices to the vicinity of this planet, *Breakthrough Starshot* will aim to address the question whether the planet hosts life by taking color photographs and potentially measuring its mass.

Our proposed interferometric accelerometer possesses a sensitivity that is superior to the Doppler technique. Furthermore, due to the interferometric nature of the proposed accelerometer, an array of $N \gg 1$ cameras would provide N^2 independent measurements instead of N if used merely for standard Doppler measurements.

The outline of the paper is as follows. In §2 we describe the Terrell effect. In §3 we discuss the application of the temporal Terrell effect in the realm of interferometry. In §4 we propose a method of measuring accelerations using such an interferometer. In §5 we describe the uncertainties inherent in the measurements and in §6 we describe various scientific utilizations of such accelerometers. Finally, we summarize our conclusions in §7.

2. THE TERRELL EFFECT

In the reference frame of a camera, located a distance $y_0 \gg R$ away from a radiating circle of rest frame radius R , the shape of the circular source is an ellipse given by

$$\gamma^2(x - vt)^2 + y^2 = R^2, \quad (1)$$

where x, y, z , and t are the camera frame 4-coordinates, v the relative velocity between the camera and the source, and γ is the corresponding Lorentz factor. Due to the finite speed of light, c , the emission time t is given by

$$t = T - \frac{y - y_0}{c}, \quad (2)$$

where T is the arrival time of the photons to the camera. Without loss of generality, we can choose a time coordinate for which $T = 0$, yielding,

$$\gamma^2(x - vt)^2 + (y_0 - ct)^2 = R^2. \quad (3)$$

This equation can be solved for $t(x)$, the time at which the photons are emitted along the circle parameterized as a function of the x coordinate,

$$t(x) = \frac{1}{c} \left\{ (y_0 + x\beta - y_0\beta^2) \pm \sqrt{(\beta^2 - 1)[(x - y_0\beta)^2 - R^2]} \right\}, \quad (4)$$

where the \pm in the square-root corresponds to light emitted from the far and near ends of the circle. The Terrell effect amounts to the fact that the (x, y) values yielding a real t solution inscribe a circle in the (x, y) plane. However, the two end points of the circle corresponding to the equation

$$(\beta^2 - 1)(x - y_0\beta)^2 - R^2 = 0, \quad (5)$$

are rotated from that of a circle at rest by an angle (see Figure 2),

$$\theta_T = \arcsin \beta. \quad (6)$$

3. THE TEMPORAL TERRELL EFFECT AND INTERFEROMETRY

Next, we shift from the point of view of the camera to that of the source. We consider an interferometric array of cameras arranged in a circle of radius R in its rest frame. This array is moving at a speed $c\beta$ in the x direction at a large distance $y_0 \gg R$ from a point source. Because electromagnetism is symmetric with respect to time reversal, this set up is exactly the same as the Terrell configuration described in the previous section, where now the "camera" is the source and the "radiating circle" is the array.

In the frame of the point source, the array is distorted into the ellipse of equation (1). However, due to the Terrell effect, the situation is equivalent to where the array stays circular but is rotated, as seen in Figure 1. This is simply equivalent to relativistic aberration: a moving source will appear as if it is oriented at a different angle.

An advantage of an interferometer array over a "photon counting" camera is that it collects phase information. This allows us to leverage a lesser known aspect of the Terrell effect. A moving circle is mapped to a rotated circle; if the circle has no features this renders Lorentz

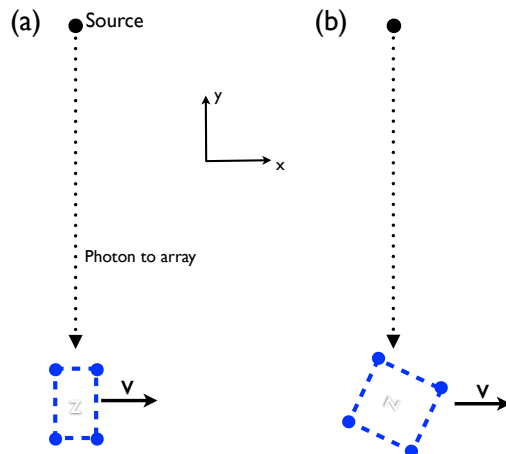


FIG. 1.— The objective (a) and apparent (b) shape of a square interferometric array in the frame of the source. The square array is Lorentz contracted, resulting in the objective shape depicted in panel (a). However, due to the Terrell effect, the apparent shape of the array is rotated by an angle $\theta_T = \arcsin \beta$. If the array would take an image of the source, the moving source would appear as if it is located at a different angle on its sky due to relativistic aberration.

contraction unphotographable. Temporal effects stemming from the Lorentz time dilation and the light travel time are, however, detectable by an interferometer.

The two end points of the circular array (where $t(x)$ has only one real solution; see Figure 2) are given by equation (5), which can be solved to yield two equations for x as a function of y_0 and β . Plugging these values of x back to equation (1) gives the arrival time of photons at these points if emitted from y_0 at $t = 0$. Labelling the leftmost point A and the rightmost point B, we can calculate the time difference between the photons arriving at A and at B (see Figure 2),

$$\Delta t = t_B - t_A = \frac{2\beta R}{c}. \quad (7)$$

Photons arriving at B have to travel for an extra time $2\beta R/c$ compared to photons arriving at A. The phase difference due to this extra travel time for electromagnetic waves with a frequency $\nu = \omega/2\pi$ and a wavelength $\lambda = c/\nu$ is

$$\phi = \omega \Delta t = \frac{2\omega\beta R}{c} = 4\pi\beta \frac{R}{\lambda}. \quad (8)$$

For an interferometric array where R/λ is of order unity, this extra phase is also of order unity at relativistic speeds with $\beta \sim 1$. However, the larger the array is (in units of wavelength), the larger would this extra phase be (modulus 2π , as with any phase measurements). Since the ratio R/λ is known, this phase measurement can be used to infer the speed, β . Combined with a measurement of angular position change, one can use this to measure the distance between the array and the source, y_0 .

4. THE TERRELL ACCELEROMETER

Based on the derivations in §3, we are now at a position to consider an accelerometer on board a spacecraft that contains no mechanical parts and is usable as long

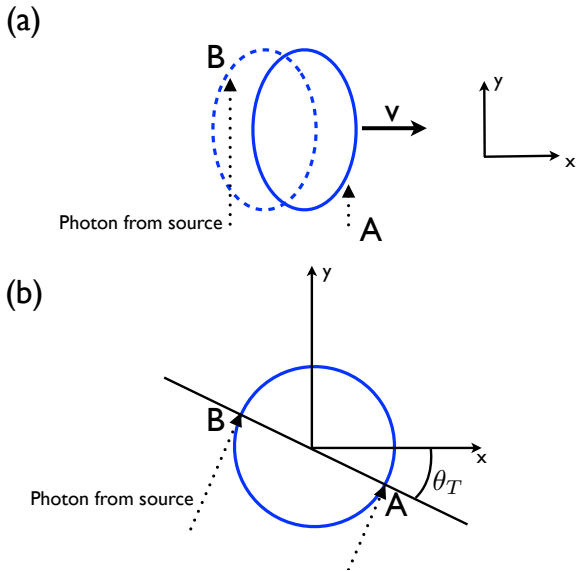


FIG. 2.— A circular array in the frame of the source (a) and its own rest frame (b). The dotted oval in panel (a) refers to the position of the array at an earlier time. In both frames, endpoints A and B satisfy equation (5). In the source frame, these points label the first photon (B) and the last photon (A) received, forming the apparent shape of the array. Photons emitted after B miss the array as it moves to the right, while photons emitted prior to A miss the array as it is not there yet. In the frame of the array the photons are emitted at an angle $\theta_T = \arcsin \beta$. Every pair of points other than A and B reflect two solutions of equation (4), for positive and negative values of y corresponding to the far and near sides of the array.

as the spacecraft's antennae are operational. If our interferometric array passes close to an object, it would be subject to gravitational acceleration. This induces a time derivative, $\dot{\beta}$, to the array's speed that could be measured. Here, we will assume the mildly relativistic regime and expand all our equations to leading order in β . Moreover, we will assume that the acceleration is small compared to the velocity during the encounter, in the sense that $c\beta \gg |\dot{\beta}y_0/c|$. Furthermore, note that $\vec{\beta}$ is oriented initially radially away from the observer.

Since the Terrell effect respects the fact that information travels at most at the speed of light, c , in reality the gravitational field should also be expanded to leading order in β . In a relativistic theory, there is no action at a distance, and the gravitational changes are transmitted at speed c . Since the gravitational field scales as $1/d^2$, where d denotes the distance between the source and the array, we find that to first order in β ,

$$\vec{g} = \left[\frac{GM(\vec{n} - \vec{\beta})}{d^2} \right]_{t_r}, \quad (9)$$

where \vec{n} is the unit vector between the array and the object, M the object's mass, G is Newton's constant, and the equation is evaluated at the retarded time $t_r = (t - d/c)$. In electrodynamics, this is the familiar equation for the electric field of a moving body as given by the Lienard-Wiechert potentials, taken to first order in β and setting the acceleration term to be small compared to the velocity term (Jackson, J. D. 1998). To lowest order, general relativity reduces to the gravitoelectric and

gravitomagnetic fields.

The \vec{n} term in equation (9) is the standard Newtonian acceleration, while the term proportional to $\vec{\beta}$ is a special relativistic term. In a flyby encounter, where the image is taken when the interferometric array and the gravitating object are at closest approach, $\vec{n} - \vec{\beta}$ evaluated at t_r points directly towards the instantaneous position of the object and is perpendicular to the instantaneous $\vec{\beta}$.

For the sake of clarity, we examine the limit of Newtonian gravity, where $t_r \rightarrow t$ and only the \vec{n} term is present. We consider a flyby where the array is passing the gravitating mass near closest approach, i.e. the x component of the velocity is much larger than the y component, $|\beta_x| \gg |\beta_y|$. Furthermore, we assume that the array is already near closest approach, where the x displacement of the object to be much smaller than its y displacement, $|x_0| \ll |y_0|$. In this case, the x component of the acceleration is given as,

$$\dot{\beta}_x = \frac{GM}{cd^2} \frac{x_0}{y_0} \approx \frac{GM}{y_0^3} \beta t. \quad (10)$$

The first derivative of equation (8) yields,

$$\dot{\phi} = 2\pi \frac{R}{\lambda} \dot{\beta}_x, \quad (11)$$

yielding a relation between the rate of change of the phase and the acceleration of the system. This gives,

$$\dot{\phi} = 4\pi \frac{R}{\lambda} \frac{GM}{cd^2} \frac{x_0}{y_0} \approx 4\pi \frac{R}{\lambda} \frac{GM}{y_0^3} \beta_x t, \quad (12)$$

As mentioned in section III, the value of y_0 can be inferred from combining the measurement of the phase, ϕ , which directly probes $\beta_x \approx \beta$ with measurements of angular acceleration, $\dot{\theta}$,

$$y_0 = \frac{c\beta}{\dot{\theta}} = \frac{c\lambda}{4\pi R\dot{\theta}} \phi. \quad (13)$$

The phase change due to the acceleration is given by the integral of equation (12) with respect to time,

$$\Delta\phi = 2\pi \frac{R}{\lambda} \frac{GM}{y_0^3} \beta_x (\tau - \tau_0)^2, \quad (14)$$

where τ is the observation time and τ_0 is an arbitrary starting time. This phase change is parabolic with respect to time; it is negative as the spacecraft approaches the gravitating body, and positive as it moves away from it. If we define $T_0 = 0$ at the point where the phase change is zero (when the spacecraft is directly in front of the gravitating body), then the mass of the body is given by

$$M = \frac{\lambda}{R} \frac{y_0^3}{GM} \frac{2\pi}{\beta_x T^2} \Delta\phi. \quad (15)$$

For an array of N antennae, this procedure can be repeated for every single baselines in the array, resulting in $N(N-1)/2$ independent measurements of the mass, M .

5. NOISE AND SYSTEMATICS

To assess the signal's detectability, we compare them to the noise inherent in the interferometer. Free from

atmosphere induced errors plaguing ground based interferometers, the fundamental phase noise of the interferometer is (Thompson, Moran, and Swenson 1986),

$$\sigma_\phi = \frac{T_S}{T_A \sqrt{2B\tau N}}, \quad (16)$$

where T_S and T_A are respectively the system and antenna temperatures, B the bandwidth, N the number of baselines, and τ the observation time. The system temperature is given in terms of the physical temperature T of the detector by (Thompson, Moran, and Swenson 1986),

$$T_S = T \left[\frac{\frac{h\nu}{k_B T}}{e^{\frac{h\nu}{k_B T}} - 1} \right], \quad (17)$$

where h and k_B are the Planck and Boltzmann constants, respectively. The antenna temperature T_A is related to the source's intensity by

$$T_A = \frac{AS}{2k_B}, \quad (18)$$

where A is the area of the antenna and S the flux density of the source. For our purposes, the point source chosen for the measurement is the Sun (as seen from the Alpha-Centauri system), N is taken to be 100, A to be 1 cm^2 , the physical temperature T to be the temperature 1 AU from a sunlike star (270 K), and the bandwidth B to be 10 percent of the frequency of observation. For such parameters, equation (19) implies a phase noise level at a wavelength of $1 \mu\text{m}$ of

$$\sigma_\phi \approx 3 \times 10^{-22} \sqrt{\frac{1 \text{ s}}{\tau N}}. \quad (19)$$

Substituting the passage time $\tau \approx d/\beta c$ as the observation time, we obtain that $\sigma_\phi \approx 10^{-22}$ for d being the Earth-Moon distance.

Within a single chip, thermal expansion causes the length of the baselines to change. Baselines between antennae located onboard different spacecrafts could also change due to orbital drifts. These phenomena generates systematic uncertainties that could be controlled by monitoring the relative positions of the antennae. This can be done by transmitting light signals between the antennae. Timing these signals allows for the distances and relative velocities between antennae to be known. In the swarm configuration where each antennae is on board a different spacecraft, either laser or the same transmission that is used to communicate back to Earth can be utilized for this purpose. In the case of multiple antennae on a single chip, optical fibers can be used as an alternative.

6. SCIENCE UTILIZATION

6.1. Weighting Stellar and planet masses

At a distance of 1 AU from a Sun-like star, the total change of phase for an array moving at $\beta = 0.2$ is given by

$$\Delta\phi \approx 3 \times 10^{-7} \times \left(\frac{R}{\lambda}\right) \times \left(\frac{1\text{AU}}{d}\right) \times \left(\frac{M}{M_\odot}\right), \quad (20)$$

where in this case we equated the observation time to the crossing time, $\tau \approx d/\beta c$. For an array of antennae

onboard the spacecrafts envisioned for the Breakthrough Starshot initiative with $R \sim 1 \text{ m}$ and $\lambda \sim 1 \mu\text{m}$, this phase change is $\Delta\phi \sim 0.3$, which is large compared to the noise described by equation (19). One could also send many antennae on separate spacecrafts, and the interferometry process can be conducted across different spacecrafts. In this case, R would be the distance between spacecrafts, allowing the use of longer wavelengths to produce the same amount of phase change.

If the spacecraft passes sufficiently close to a planet, the gravitational pull of the planet would dominate over that of its parent star. For a planetary system similar to the Sun-Earth system, this would occur when the planet-spacecraft separation is about $3 \times 10^{10} \text{ cm}$, or roughly the Earth-Moon distance. In such a flyby, the total change of phase at $\beta = 0.2$ is given by

$$\Delta\phi \approx 4.7 \times 10^{-10} \times \left(\frac{R}{\lambda}\right) \times \left(\frac{3 \times 10^{10} \text{ cm}}{d}\right) \times \left(\frac{M}{M_\oplus}\right), \quad (21)$$

which gives $\Delta\phi \sim 4.7 \times 10^{-4}$ for the configuration with $R \sim 1 \text{ m}$ and $\lambda \sim 1 \mu\text{m}$. This phase difference is large compared to the noise described by equation (19). This will complement an alternative measurement of the planet's mass that is enabled by sending a spacecraft to the system, such as by determining the orbital inclination of the planet by resolving the planet's orbits as the spacecraft approaches the planetary system.

We note that it is not necessary to use the star or planet as the light source. If the array is focused on some distant point source like the Sun, the acceleration of the detector will still be apparent. However, if the star or planet is used as the light source, its resolved image can be viewed as a collection of point sources, and each of them will suffer the same temporal drift in phase due to the acceleration. The observer would see each pixel in the u-v plane of the interferometer drifting in time. This will also enable a measurement of the acceleration.

6.2. Measuring density profiles of planetary systems

Approaching the target star system with antennae allows one to measure the enclosed mass of the system as a function of distance from the star. In particular, this allows to measure the cumulative mass of Kuiper belt analogs in the target system. At a distance of 30 AU, a Kuiper belt analog of combined mass $\sim 30M_\oplus$ produces an extra acceleration of

$$c\dot{\beta} = \frac{30GM_\oplus}{(30 \text{ AU})^2}, \quad (22)$$

which translates into an additional phase change of

$$\Delta\phi \approx 10^{-12} \times \left(\frac{R}{\lambda}\right) \times \left(\frac{30\text{AU}}{d}\right) \times \left(\frac{M}{30M_\oplus}\right). \quad (23)$$

For the configuration with $R \sim 1 \text{ m}$ and $\lambda \sim 1 \mu\text{m}$, this phase change becomes $\sim 10^{-6}$, which is above the noise implied by equation (19).

6.3. Measuring the Milky Way mass

Travel to the closest star from Earth requires an extended period of time for the journey. At $\beta = 0.2$, it will take roughly 20 years to travel from Earth to Alpha-Centauri. During this travel time, one can use the phase

change of any source to weight the Galactic mass. The current estimate for the enclosed Milky Way mass at the distance of 8 kpc from the Galactic center is $\sim 10^{11} M_{\odot}$ (Reid et al. 2014); therefore,

$$\Delta\phi \approx 10^{-30} \times \left(\frac{R}{\lambda}\right) \times \left(\frac{T}{\text{sec}}\right)^2. \quad (24)$$

Although this number is small, the travel time is longer than in the case considered in §4.1. If measurements are taken for the full travel time of ~ 20 years to Alpha-Centauri, the total phase change is,

$$\Delta\phi \approx 3 \times 10^{-15} \left(\frac{R}{\lambda}\right). \quad (25)$$

This will provide a phase change of unity for $\lambda \sim 1\mu\text{m}$ if $R \sim 10^9$ cm. While the phase change for the $R \sim 1$ m configuration is small, note that it is still large compared to the noise described by equation (19) provided that the Sun could be used as the point source in the experiment.

6.4. Testing modified gravity

Long distance modifications of gravity could be constrained by monitoring the acceleration of the spacecraft (Buscaino et al. 2015; Hees et al. 2014; Kalinowski, M. W. 2015). These modifications could be parameterized by adding a Yukawa term to the usual $1/r$ gravitational potential,

$$\Phi(r) = -\frac{GM}{r} \left[1 + \alpha e^{-r/l}\right] \quad (26)$$

$$\approx -\frac{GM}{r} \left[1 + \alpha - \frac{\alpha r}{l} + \frac{r^2}{2l^2} + \dots\right], \quad (27)$$

where α is the strength of the Yukawa force and l is the characteristic length-scale at which the gravitational force is substantially modified from $1/r^2$. As noted in Buscaino et al. (2015), the zeroth order correction is simply a rescaling of the mass and the first order correction is a constant shift in the potential. The lowest order observable term is second order in (r/l) and produces the constant acceleration

$$\delta a = \frac{\alpha GM}{2l^2}, \quad (28)$$

where we use δ to signify the difference in physical quantities between the cases with and without the Yukawa interaction. Modifying equation (10) by this term yields the difference between the x -accelerations of $1/r^2$ and Yukawa gravity to be

$$\delta\dot{\beta}_x = \frac{\alpha GM}{c^2 l^2} \frac{x_0}{y_0} \approx \frac{GM}{l^2 y_0} \beta t. \quad (29)$$

This produces a total phase shift of,

$$\delta\phi = 2\pi \frac{R}{\lambda} \left(\frac{\alpha GM}{l^2}\right) \frac{d}{\beta c^2}, \quad (30)$$

where d is the distance to the source and again we equated the observation time to the crossing time, $d/\beta c$. Placing the detectors at multiple distances from a star, the strength of the Yukawa potential, α can then be directly measured. The smallest phase shift measureable is given by (19), implying that the experiment is sensitive to measure α down to,

$$\alpha_{min} = \sigma_{\phi} \frac{l^2}{GM} \left(\frac{\beta c^2}{d}\right) \frac{\lambda}{2\pi R}. \quad (31)$$

For a Yukawa potential with length-scale $l \sim 100$ AU, a detector located at $y_0 \approx l$ around a sun-like star can measure α down to

$$\alpha_{min} \approx 2 \times 10^{-17} \times \sqrt{\frac{100}{N}} \times \frac{\lambda}{R}, \quad (32)$$

where N is the number of baselines in the measurements. With 10 antennae, the number of baselines becomes $N \approx 100$, allowing the measurement of α_{min} to a few orders of magnitudes better than state of the art experiments (Buscaino et al. 2015). In addition to its sensitivity, another benefit for using this method is that one can test the long range modification of gravity on much larger scales than previously possible.

7. CONCLUSION

We showed that the temporal Terrell effect provides an exquisite probe of acceleration for an interferometric array traveling at a relativistic speed. In the context of the envisioned parameters of the Breakthrough Starshot spacecraft ($R \sim 0.1 - 4$ m, $\lambda \sim 1\mu\text{m}$, $\beta \sim 0.2$), equations (20) and (21) imply measureable phase variations for a Sunlike star and an Earth mass planet, respectively. An interferometric array of N elements onboard such a spacecraft could provide $N(N-1)/2$ measurements of the mass, allowing a new observational method for measuring masses and testing theories of modified gravity in astronomy.

8. ACKNOWLEDGEMENT

The authors thank Michael Johnson and Martin Rees for comments on the manuscript and an anonymous referee for insightful suggestions. This work was supported in part by a Starshot grant from the Breakthrough Prize Foundation to Harvard University and by NSF grant AST-1312034.

REFERENCES

- Terrell, J. 1959, *Physical Review*, 116, 1041-1045
 Penrose, R. 1959, *Proceedings of the Cambridge Philosophical Society*, 55, 137-139
 Hollenbach, D. 1976, *American Journal of Physics*, 44, 91
 Scott, G. D. and van Driel, H. J. 1970, *American Journal of Physics*, 38, 971
 Suffern, K. 1988, *American Journal of Physics*, 56, 729
 Sheldon, E. 1989, *American Journal of Physics*, 57, 487
<https://breakthroughinitiatives.org/Concept/3>
 Anglada-Escude, G. et al. 2016, *Nature*, August 25 issue, 2016
 Schneider J., Dedieu, C., Le Sidaner, P., et al. 2011, *A&A*, 532, A79
 Jackson, J. D. 1998, *Classical Electrodynamics* 3rd Edition, Wiley
 Reid, M., Menten K. M., Brunthaler, A., et al. 2014, *ApJ*, 783, 130
 Buscaino, B., DeBra, D., Graham, P. W., Gratta, G., et al., 2015, *Physical Review D*, 92,10,104048
 Hees, A., Folkner, W. M., Jacobson, R. A., Park, R. S., 2014, *Physical Review D*, 89, 10, 102002
 Kalinowski, M. W., 2015, *Fortschritte der Physik*, 63, 711-918

A. R. Thompson, J. M. Moran, and G. W. Swenson. 1986,
Interferometry and synthesis in radio astronomy.